An Efficient Power Management Algorithm for a Micro Grid

B.Sireesha*, Y.Nagaraja
Departement of Electrical and Electronic Engineering,
Annamacharya Institute of Technology & Sciences (AITS), Kadapa, India
*Corresponding author, e-mail: sireesha.reddy00@gmail.com

Abstract
This paper displays a micro grid comprising of distributed generation (DG) units (DG) units that are joined with the conveyance framework. A vitality administration calculation is actualized to arrange the operations of the various DG units in the micro grid for framework joined during grid connected and islanded operations. The proposed micro grid comprises of a photovoltaic (PV) cluster which works as the essential era unit of the micro grid furthermore a proton-trade layer energy component to supplement the variability in the force produced by the PV show. A lithium-particle capacity battery is joined into the micro grid to alleviate top requests amid lattice associated operation and to adjust for any lack in the created force amid islanded operation.The outline idea is checked through different test situations to exhibit the operational capacity of the proposed micro grid, and the acquired results are talked about.
Keywords: PaperDistributed Generation, Power Management, Micro Grid.

1. Introduction

Micro grids are distribution systems with DG units, energy storages and controllable loads, which can be operated parallel with utility grid or in an island mode. Micro grid can be disconnected from the utility grid as a consequence of disturbances in the utility grid or due to planned switching events an increasing demand for the reliable, high quality power and an increasing number of distorting loads have led to an increased awareness of power quality both by customers and utilities.

In addition, most of the distributed generation (DG) units connected in future to low voltage (LV) network micro grids will be converter based. These DG unit converters together with possibly existing nonlinear loads have potential to distort the voltage waveform even more. This paper studies the voltage and current THD before and after islanding in the micro grid with different micro grid configurations. The basic structure of the present day power system is the integration of generation, transmission and distribution system. In conventional power plants, electricity is produced from fossil fuels such as coal, oil and natural gas and these generating stations will be located far away from the load centers due to safety concern and due to the availability of energy sources. Power generated from these stations are then transmitted over long distance at high voltage levels to the load centers and then delivered to the customer load points with the help of sub-transmission networks and distribution networks. This leads to the higher transmission losses and also the complexity of the system increases. Also, the environmental effects caused by these fossil fuels are high due to their high carbon emission. As a result, renewable energy resources such as wind, tidal, solar, small hydropower and biomass are becoming the best option for generating electric power due to their low environmental effects.

The current power system is undergoing considerable amount of changes, because more renewable energy based power conversion systems are connected to the low voltage distribution systems as distributed generators due to their environment friendliness and reliability. On the other hand, dc loads such as LED lights, refrigerators and electric vehicles are increasing to save electric energy and to reduce emissions. In the present system, these loads are supplied by means of AC power sources along with the help of power electronics converters. This further increases the cost of the system and appliances as it requires additional converters. When power can be supplied by renewable energy based distributed generators, there is no need for high voltage transmission and also transmission losses can be reduced. AC

micro grids have been developed to enable the connection of renewable energy based power generating sources to the present AC system. As stated earlier, due to increasing amount of DC loads in residential, industrial and commercial buildings the power system loads are becoming DC dominated. In many industries DC power is required for the speed control purpose. If these loads are supplied by means of AC grid, then it requires embedded AC/DC converters and DC/DC converters to supply different DC voltages. As a result [1], DC grids are resurging due to the various advantages of renewable energy sources and their inherent advantage of supplying DC loads. The multiple reverse conversions associated with an individual ac or dc grid leads to additional costs and losses and hence reduces the overall efficiency of the system. A hybrid AC/DC micro grid helps to minimize these multiple reverse conversion problem which normally associated with individual AC grids or DC grids. In this hybrid system AC loads are connected to the AC grid and DC loads are connected to the DC grid and the AC and DC grids are connected through a bidirectional converter. The proposed architecture, operation and control of the hybrid micro grid are more complicated than those of individual DC grid or AC grid [2-3]. The various control mechanisms for controlling the converters and to maintain the stable system operation in grid connected mode is explained in the following sections.

2. Modeling of Proposed Micro Grid

Figure 1 shows the configuration of the micro grid proposed in this paper that is designed to operate either in the grid-connected or islanded mode. The main DG unit comprises a 40-kW PV array and a 15-kW PEMFC, which are connected in parallel to the dc side of the DG inverter -1 through dc/dc boost converters to regulate the dc-link voltage of the DG inverter at the desired level by delivering the necessary power. The PV array is implemented as the primary generation unit and the PEMFC is used to back up the intermittent generation of the PV array. When there is ample sunlight, the PV array operates in the MPPT mode to deliver maximum dc power , which is discussed in detail in [3] and [4], and the output voltage of the PV array is permitted to vary within an allowable range to ensure proper operation of the DG inverter. To maintain the level of the dc-link voltage at the required level, the PEMFC supplements the generation of the PV array to deliver the necessary. When the output voltage of the PV array falls below a preset limit, PV array is disconnected from the DG unit and the PEMFC functions as the main generation unit to deliver the required power. A30-Ah lithium-ion SB is connected to the dc side of DG inverter- 2 through a bidirectional dc/dc buck-boost converter to facilitate the charging and discharging operations.. The role of the main DG unit functions to provide local power and voltage support for the loads and, hence, reduces the burden of generation and delivery of power directly from the distribution grid.
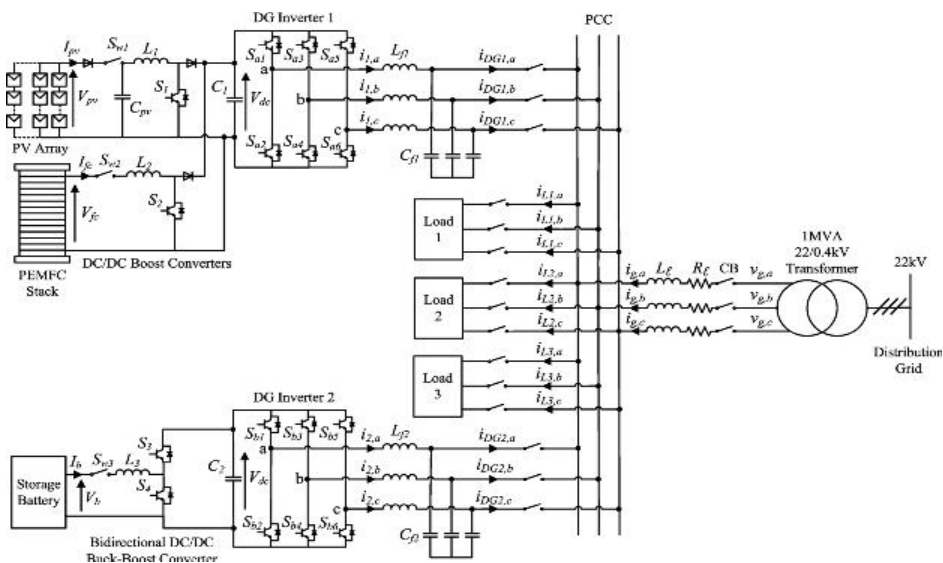

Figure 1. Overall configuration of the proposed micro grid architecture

During islanded operation, the role of the SB is to maintain the power balance in the micro grid which is given by:

$$P_{DG} + P_b = P_L \qquad (1)$$

Where PDG is the power delivered by the main DG unit, & Pb is the SB power which is subjected to the charging and discharging constraints given by:

$$P_b \qquad P_{b,max} \qquad (2)$$

And PL is the real power delivered to the loads. The energy constraints of the SB are determined based on the state-of-charge (SOC) limits which are given as:

$$SOC_{min} < SOC \qquad SOC_{max}. \qquad (3)$$

Although the SOC of the battery cannot be measured directly, it can be determined through several estimation methods presented in [5] and [6]. When the micro grid operates islanded from the distribution grid, the SB can operate in the charging, discharging, or idle mode depending on its SOC.
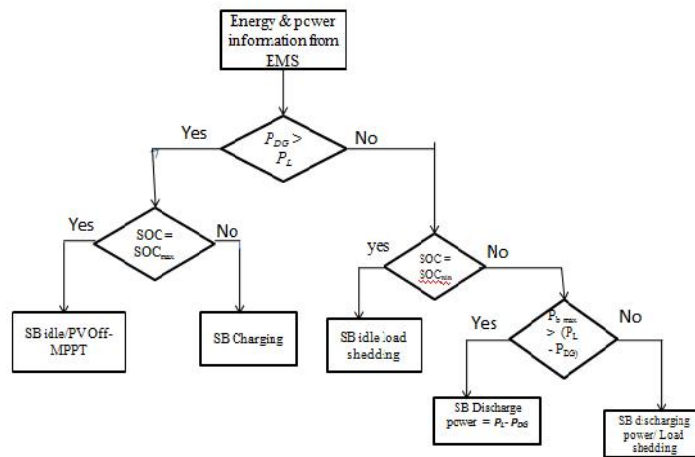

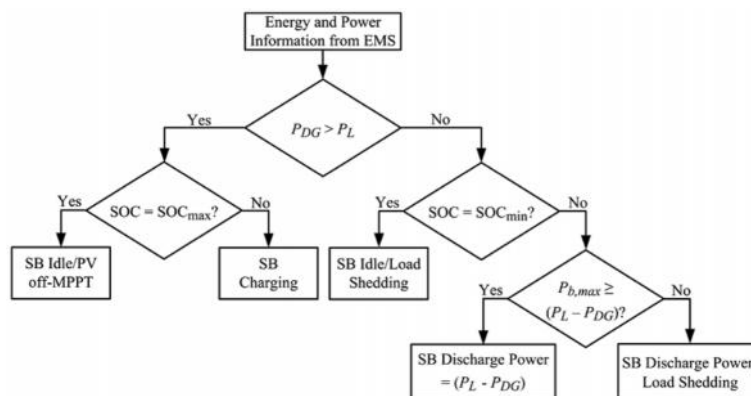Figure 2. Operation of the SB during grid-connected operation

Fig. 3. Operation of the SB during islanded operation

The flowcharts in Figure 2 and 3 summarize the operation of the SB during grid connected and islanded operation as shown in figure. SB can be operated based on the output information provided by an energy-management system (EMS) during grid-connected and

islanded operation, respectively. The EMS controls and monitors different aspects of power management, such as load forecasting, unit commitment, economic dispatch. During grid-connected operation, the distribution grid is connected to the micro grid at the point of common coupling (PCC) through a circuit breaker (CB). With the proliferation of power-electronics equipment being connected to the micro grid, the load currents could be distorted due to the presence of harmonic components.

The DG units also function to compensate for any harmonics in the currents drawn by nonlinear loads in the micro grid, so that the harmonics will not propagate to other electrical networks connected to the PCC. Generally, there are variations in the power generated by the PV array and that demanded by the loads [7]. If the power generated by the main DG unit is greater than the total load demand in the micro grid, the excess power can be used to charge the SB or injected into the distribution grid, depending on the SOC of the SB, Conversely, when the total load demand is greater than the power generated by the main DG unit, the SB can be controlled to achieve different energy-management functions depending on its SOC and the time of use (TOU) of electricity. When the cost of generation from the grid is low and if the SB's SOC is below the maximum SOC limit SOCmax & the SB can be charged by the grid and the loads will be supplied by the main DG unit and the grid. During peak periods, when the cost of generation from the grid is high and if the SB's SOC is above the minimum SOC limit SOCmini, the SB can deliver power to the grid to achieve peak saving.

When a fault occurs on the upstream network of the distribution grid, the CB operates to disconnect the micro grid from the distribution grid. The main DG unit and the SB are the sole power sources left to regulate the loads. In the case when the generation capacity of the main DG unit is unable to meet the total load demand, the SB is required to provide for the shortage in real and reactive power to maintain the power balance and stability of the micro grid as shown in Figure 3. When the total load demand exceeds the generation capacity of the main DG unit and the SB, the EMS detects a drop in the system frequency and load shedding for noncritical loads is required to restore the system frequency and maintain the stability of the micro grid [8].

3. Single Phase Representation of DG Inverters
3.1. Grid connected operation

Figure 4 and 5 shows the equivalent single-phase representation of the DG inverters for grid-connected and islanded operation The total load current iL, which is the sum of the currents delivered to the load K (K=1 , 2, 3), is given by:
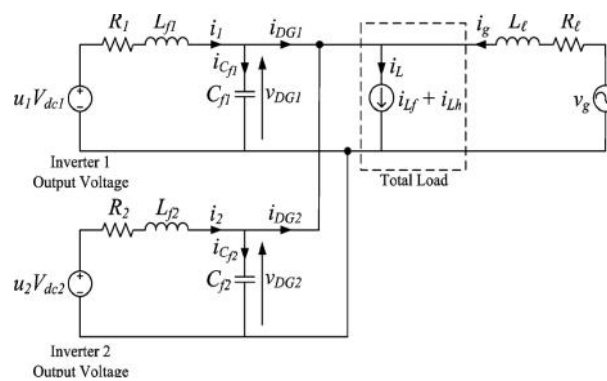
$$i_L = i_{L1} + i_{L2} + i_{L3} \tag{4}$$

Figure 4. Equivalent single-phase representation of the DG inverters for grid connected operation

And IL can be modelled as two components consisting of fundamental iLf and harmonic iLh with their peak amplitudes ILf and ILh, respectively, and is represented by:

$$i_L = i_{Lf} + i_{Lh} = I_{Lf}\sin(wt - \phi Lf) + \sum_{h=3,5..}^{N} I_{Lh} \sin(hwt - \phi_{Lh})$$
$$= I_{Lf}\sin wt \cos \phi Lf - I_{Lf}\cos wt \sin \phi Lf + \sum_{h=3,5..}^{N} I_{Lh} \sin(hwt - \phi_{Lh})$$
$$= i_Lf,p + i_Lf,q + i_{Lh} \tag{5}$$

Where ϕ_{Lf}, ϕLh are the respective phase angles of the fundamental and harmonic components of i_L and $i_{Lf,p}$ and $i_{Lf,q}$ are the instantaneous fundamental phase and quadrature components of i_L. To achieve unity power factor at the grid side, compensate for the harmonics in the load currents and concurrently achieve load sharing, the inverter of the DG unit supplies a current iDGj that is given by:

$$i_{DGj} = (i_{Lf,p} - ig) + i_{Lf,q} + i_{Lh} \tag{6}$$

Where ig is the grid current. The distribution grid is supplied by a utility substation represented by a voltage source vg during grid-connected operation, and is connected to the micro grid and the loads via a distribution line with resistance Rl and inductance Ll as shown in Figure 4.

In the grid-connected mode, the micro grid shares the load demand with the grid. Hence, to control the power delivered to the loads, the output current of the DG inverter is controlled using the current control mode (CCM).

3.2. Islanded Operation
During islanded operation, the micro grid will supply the overall load demand as shown in Figure 5, and it is required that the output voltage be regulated to a pure sine wave with a fixed magnitude. This can be achieved through the voltage-control mode (VCM).
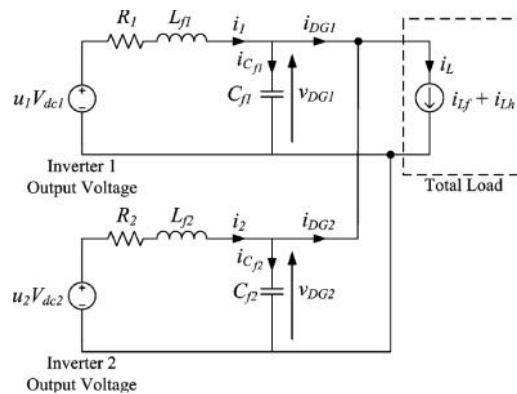

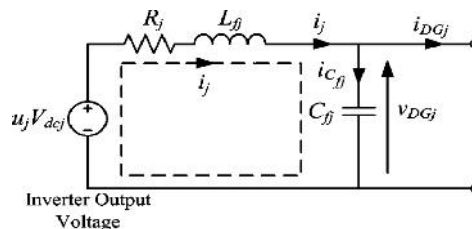Figure 5. Equivalent single-phase representation of the DG inverters for islanded operation

Figure 6. Single-phase representation of the jth DG inverter for grid-connected & islanded operations

To derive a state-space model for the DG inverter during both grid-connected and islanded operations, Kirchhoff's voltage and current laws are applied to the current loop as shown in Figure 6, and the following equations are obtained.

$$\frac{dij}{dt} = -\frac{Rj}{Lfj}ij - \frac{1}{Lfj}VDGj + \frac{Vdcj}{Lfj}uj \tag{7}$$

$$\frac{dvDGj}{dt} = -\frac{1}{Cfj}ij - \frac{1}{Cfj}iDGj \tag{8}$$

Where ij is the current passing through Lfj. Hence, the grid connected DG inverter model can be written as:

$$_{gj} = A_{gj}x_{gj} + B_{gj1}v_{1j} + B_{gj2}u_j \tag{9}$$

$$y_{gj} = C_{gj}x_{gj} + D_{gj1}v_{1j} + D_{gj2}u_j \tag{10}$$

Where the subscript g and j represent the model of DG inverter j during grid-connected operation (j = 1,2) and:

$$Agj = -\frac{Rj}{Lfj} \; ; B_{gj1} = [\frac{1}{Lfj} \quad 0] \; ; B_{gj2} = \frac{Vdcj}{Lfj} \; ; C_{gj} = 1$$

$$D_{gj1} = [0 \; -C_{fj}]; D_{gj2} = 0$$

$Xgj = ij$ is the state; $V1j = [vDGj \; \frac{dvDGj}{dt}]T$ is the exogenous input; uj = Control input, with -1 ≤ uj ≤ 1; and ygj = iDGj is the output. During islanded operation, the frequency will change due to power imbalance in the micro grid. This change in frequency is detected by the EMS of the micro grid, which is used to manage and monitor the power dispatch by each DG unit. Based on the frequency change information, the EMS will require the main DG unit and the SB to generate the necessary power to meet the overall load demand in the micro grid as shown in the flowchart of Figure 3, such that (1) satisfied. During islanded operation, it follows from (7) and (8) that DG inverter can be modelled as:

$$_{ij} = A_{ij}x_{ij} + B_{ij1 \; j} + B_{ij2}u_j \tag{11}$$

$$y_{gj} = C_{ij}x_{gj} + D_{ij1 \; j} + D_{ij2}u_j \tag{12}$$

Where the subscript i denotes the model of the DG inverter j during islanded operation (j=1 , 2) and:

$$Aij = \begin{bmatrix} -\frac{Rj}{Lfj} & -\frac{1}{Lfj} \\ \frac{1}{C1f} & 0 \end{bmatrix} \; ; Bij = -\frac{0}{\frac{1}{c1f}}$$

$$B_{ij2} = \frac{Vdcj}{Lfj}\\0 \quad C_{ij} = \begin{bmatrix} 0 & 1 \\ 1-\frac{Cfj}{C1f} & 0 \end{bmatrix} \; ; D_{ij1} = \frac{0}{-\frac{cfj}{c1f}} \; ; D_{ij2} = \frac{0}{0}$$

Here, xij = state vector i1j = exogenous input; uj = control input, with -1 ≤ uj ≤ 1; yij = output, which will be regulated to track the desired reference waveform. Both VDGj and iDGj will be regulated in the VCM to safeguard that the power is delivered. Furthermore, it is assumed that the exogenous input i1j, in the model is not directly measurable by the DG inverter j since it involves quantities outside that inverter. Precisely, i1j represents the sum of all load currents iL minus the sum of all in from the other DG inverters in the micro grid. Although only one other inverter has been presented in the proposed micro grid, the model is extendable to more DG inverters.

4. Proposed Controller
This paper proposes a novel MPC algorithm for the control of the DG inverters of the micro grid. The proposed algorithm is specifically designed for fast-sampling systems, to track

periodic signals so as to deal with the dual-mode operation of the micro grid. The algorithm decomposes the MPC optimization into a steady-state sub-problem and a transient sub-problem. Furthermore, the steady-state sub problem adopts a dynamic policy approach in which the computational complexity is adjustable. The decomposition also allows the steady-state sub-problem to be solved at a lower rate than the transient sub-problem if necessary. These features help to achieve a lower computational complexity and make it suitable for implementation in a fast-sampling system like our micro grid applications. In the simulation studies in this paper, the sampling interval is chosen as 0.2ms, which is considered pretty small in conventional MPC applications, but necessary for the high order of harmonics being tackled for our problem. Sampling in the range of tens of kHz is possible with state-of-the-art code generation techniques [9-10].

It is noted that in either the grid-connected or the islanded operation, the state-space model will take the form:

$$X+ = Ax + B_1w + B_2u \tag{13}$$

$$Y = Cx + D_1w + D_2u \tag{14}$$

Where the superscript + represents the time-shift operator (with sampling interval Ts), and the exogenous signal   is periodic. In general, any periodic signal with a finite number of harmonics can be written as the output of an autonomous finite-dimensional linear time-invariant state-space model. For example, if the periodic signal has a fundamental frequency   and consists of only odd harmonics, the A-matrix of the corresponding state-space model can take a block diagonal form with the blocks given by:

$$\begin{bmatrix} \cos h\,Ts & \sin h\,Ts \\ \sin h\,Ts & \cos h\,Ts \end{bmatrix}$$

Where h= 1,3,5,… and the C- matrix [1 0 1 0 …1 0].Hence the exogenous signal   in (13) and (14) together with reference d that y in (14) desires & can be modelled by:

$$+ = A \tag{15}$$

$$= C \tag{16}$$

$$d = Cd \tag{17}$$

The state-space model given by (15)-(17) is known as the exogenous system in this paper. Although only odd harmonics up to the 29th order have been considered, the methodology can be easily extended to include even harmonics [11-12]. The exogenous state , which essentially represents the sets of Fourier coefficients of   and d, can be automatically identified using a Kalman-based observer known as the exogenous Kalman filter once the signal   is measured and the reference d is specified. The exogenous Kalman filter is given by

$$+ = A + L (-) + Ld (d - d\sim) \tag{18}$$

$$= C \tag{19}$$

$$d = Cd \tag{20}$$

The control in (13) and (14) is decomposed into a steady-state control us and a transient control ut as:

$$U = u_s + u_t \tag{21}$$

The controller can solve steady state sub problems and transient state sub problems.

4.1. Steady-State Sub problem

The control objective of the steady-state sub problem is to identify an optimal control signal us such that when u   us asymptotically and, thus x   xs and y   ys. According to (13) and (14), us , xs and ys should satisfy:

$$X_{s+} = Ax_s + B_1w + B_2u_s \qquad (22)$$

$$y_s = C x_s + D_1w + D_2u_s \qquad (23)$$

Subject to the constraint that:

$$Us \quad 1 \qquad (24)$$

4.2. Transient Sub Problem

Us, Xs and Ys are identified by the steady-state sub problem, the control objective of the transient sub problem is to ensure that the transient signals ut = u-us, xt=x-xs, and y=y-ys will go to zero. Then according to (13) and (14), and (22) and (23), ut , xt and yt should satisfy:

$$X_{t+} = Ax_t + B_2u_t \qquad (25)$$

$$Y = Cx_t+D_2u_t \qquad (26)$$

In this the objective is to make yt   0 , the constraint is:

$$u_s + u_t \quad 1 \qquad (27)$$

A conventional approach of MPC that employs a finite horizon with a terminal cost can be adopted. It requires the information of us and xs, which will be provided by the information of the plant state x, which can be estimated using a plant Kalman filter on (13) and (14)
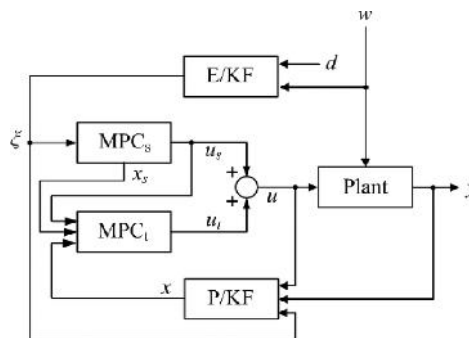

Figure 7. Overall MPC controller for the DG inverter E/KF denoting the exogenous Kalman filter andP/KF denoting the plant Kalman filter

Table 1. Parameters of the proposed system

Parameter	Value
Distribution grid voltage	v_g =230V (phase)
DC link voltage	V_{dc} =400V
Distribution line impedance	R_ℓ = 0.0075Ω, L_ℓ = 25.7μH
LC filter	L_f= 1.2mH, C_f = 20μF
DG inverter loss resistance	R_f =0.01 Ω

The micro grid is tested under various conditions to evaluate its capabilities when operating connected and islanded from the distribution grid. Three different load types consisting of linear and nonlinear loads are considered in the studies [13-14]. For load 1, a 15-kVA three-phase PWM adjustable speed drive (ASD) with its configuration as shown in Figure 8 is used and load 2 is made up of a three-phase RL load rated at PL2 = 28 kW and QL2 = 18.5 kVAR. Load 3 is a noncritical three-phase dimmer load rated at PL3 = 18 kW and QL3 = 12.3 kVAr, which is nonlinear in nature and will be shed under emergency conditions when the generation of the micro grid is unable to meet the load demand. The per-phase currents iL1 , iL2 and iL3 drawn by loads 1, 2, and 3 for 0   t < 0.2 s are shown in Figure 9. The system parameters are given in Table 1.
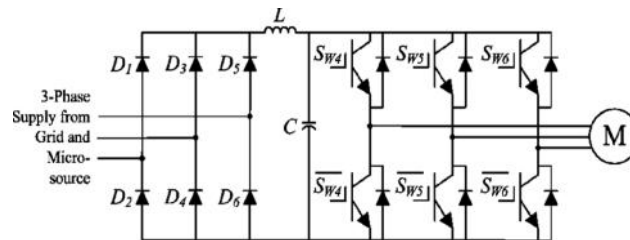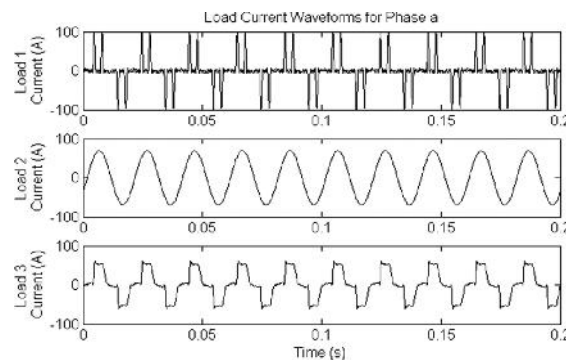

Figure 8. Configuration of a 15-kVA three-phase ASD

5. Simulation Studies

The simulation model of the micro grid shown in Figure 1 is realized in Matlab/Simulink. The micro grid is tested under various conditions to evaluate its capabilities when operating connected and islanded from the distribution grid. Three different load types consisting of linear and nonlinear loads are considered in the studies.

Figure 9. Per-phase currents drawn by loads 1, 2, and 3

Test Case 1: Power Quality Improvement WithLoad-Sharing During Grid-Connected Operation:
The first test case demonstrates the capability of the micro grid to improve the power quality of the distribution network by compensating for the harmonics in the total load current due to the nonlinear loads that are connected to the distribution network. In this test case, the main DG unit accounts for 20% of the total load demand. The waveforms of the total load current, the current supplied by the main DG unit iDG and grid current ig under this test case are shown in Figure 10. The unsteady measurements in iDG and ig as shown in Figure 10 (middle) and Figure 10 (bottom)respectively during initialization for 0   t < 0.06 s are due to the fact that the controller needs

A period of 3 cycles to track the generated references. During steady-state condition, the total harmonic distortion (THD) value of iL is 42.1% as shown in Figure 12 (top). With the

main DG unit compensating for the harmonic currents as shown in Figure 10 (middle), the THD value of ig is improved to about 0.4% as shown in Figure 10 (bottom). To achieve power factor correction at the grid side, the main DG unit is also controlled to provide the reactive component i Lf,q of the current iL given in (5).

Figure 11 shows closed-up waveforms of the grid voltage vg and ig of phase a for 0.2 t < 0.24s. It is observed that the waveform of ig is in phase with that of vg with power factor correction.

Figure 10. Waveforms of three-phase load current (top) iL, three-phase DG current iDG (middle), and three-phase grid current ig (bottom)
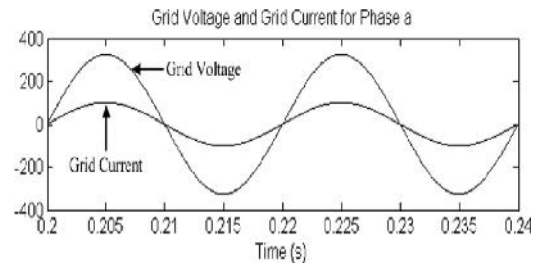
Figure 11. Grid voltage vg and grid current ig for phase a

The total real and reactive power delivered to the loads isabout 58 kW and 35 kVAR as shown in the power waveforms of Figure 12.
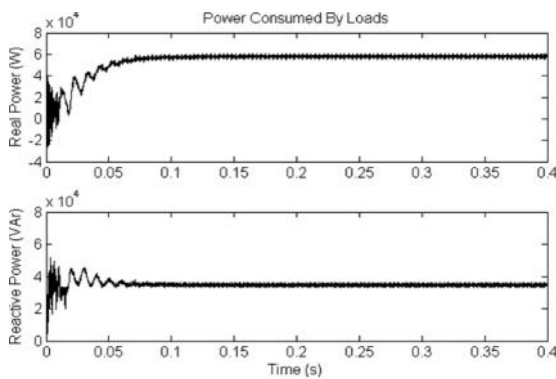

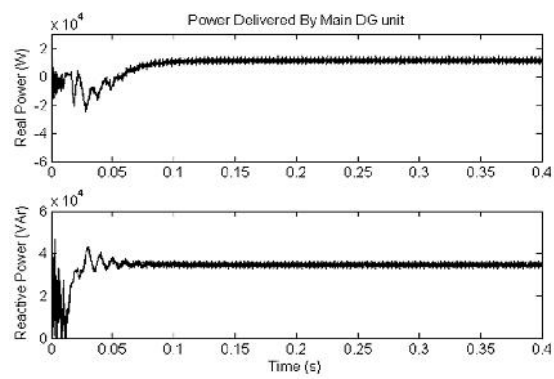Figure12. Real (top) and reactive (bottom) power consumed by loads

Figure 13. Real&reactive power delivered by main DG unit

The real power dispatched by the main DG unit is 11.6 kW (20% of the real power consumed by the loads) as shown in Figure 13, which demonstrates the capability of the main DG unit to dispatch the required power. The main DG unit also delivers all of the reactive power required by the loads to achieve unity power factor at the grid side. The real and reactive power delivered by the grid is shown in Figure 14. It can be observed from Figure 14 that the grid supplies 80% (46.4 kW) of the total real power delivered to the loads and dispatches an additional power of about 3 kW to charge the SB. It is also observed that the reactive power supplied by the grid is zero, resulting in unity power factor at the grid side.
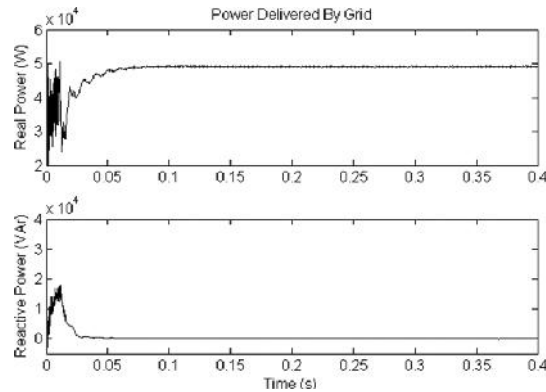
Figure 14. Real (top) and reactive (bottom) power delivered by the grid

Test Case 2: Peak Shaving of Loads During Peak Periods

The second test case demonstrates the operation of the micro grid to achieve peak shaving in order to reduce the cost of generation from the grid when consumers practice DSM. The power waveforms of the grid for 0 t < 0.4 s are shown in Figure 15. It can be seen that the real power delivered by the grid is 60% (34.8 kW) of the load demand with peak shaving, and the reactive power supplied is zero with the main DG unit compensating for the reactive components of the load currents. The real power waveform delivered by DG inverter-2 (as shown in Figure 1) of the SB during discharging is shown in Figure 16. It can be observed from Figure 16 that the SB delivers the required real power of about 20% (11.6 kW) of the load demand during peak shaving.
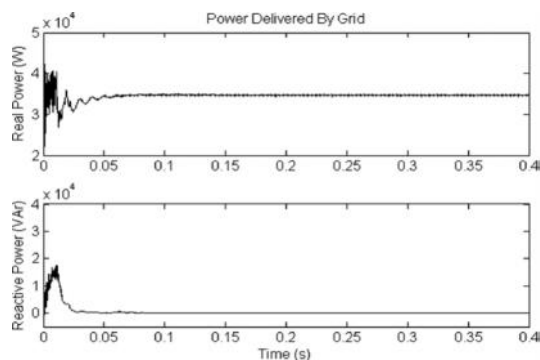

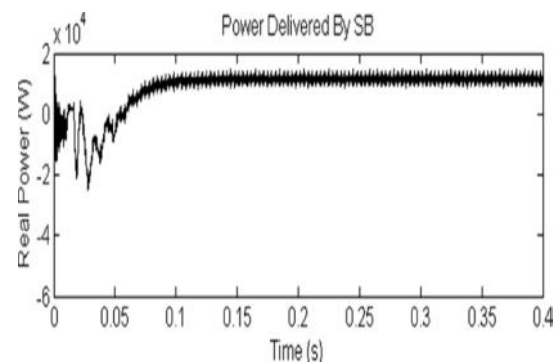Figure 15. Real (top) and reactive (bottom) power delivered by the grid

Figure 16. Real power delivered by SB

Test Case 3: Load Shedding During Islanded Operation

The third test case demonstrates the operation of the micro grid when it islands from the grid. In this test case, the micro grid is initially operating in the grid-connected mode for 0 t < 0 0.2 s. The SB is initially operating in the idle mode and its SOC is 80%. A fault occurs on the upstream network of the micro grid is disconnected from the distribution grid at 0.2 s. Figure 17 shows the waveforms of the real and reactive power supplied by the grid. It can be seen that the CB manages to fully isolate the micro grid from the distribution grid in about half a cycle, resulting in zero real and reactive power delivered by the grid for 0.2 t < 0.6 s. The real power delivered by DG inverter 2 of the SB is shown in Figure 18. For 0 t < 0.2s, the SB is in the idle mode. After the initiation of the islanding operation at t = 0.2 s, the DG inverter 2 is tasked by the EMS to increase its generation to provide real power of about 12.5 kW to the loads. The main DG unit and the SB supplying for the loads, the power imbalance results in a decrease in the system frequency, which is detected by the EMS. To maintain the stability of the micro grid

during islanded operation, the shedding of load 3 (18 kW and 12.3 kVAr) is also initiated at 0.4 s by the EMS such that the total generation from the main DG unit (27.5 kW and 22.7 kVAr) and the SB (12.5 kW) can meet the power demand by the loads. A delay of 0.2 s is introduced between islanding of the micro grid and load shedding to cater for frequency transients that might occur momentarily due to the energization of large motor loads. The waveforms of the real and reactive power delivered to the loads for 0 0.6 s are shown in Figure 19. It can be observed that when load 3 is shed at 0.4 s, the total real and reactive power delivered to the loads gradually decreases to settle and operate stable at about 40 kW and 22.7 kVAr, respectively, in about 3 cycles.
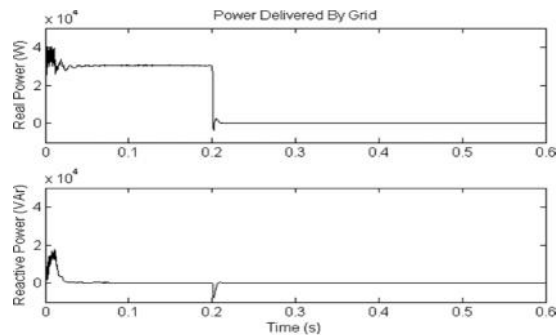

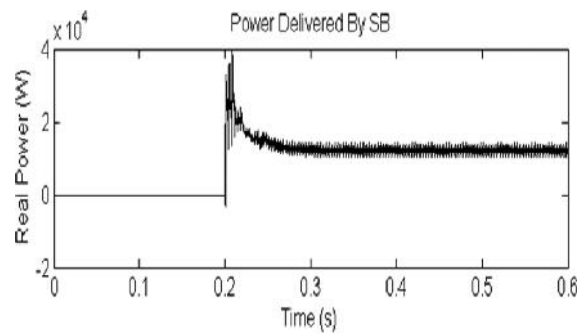Figure 17. Real (top) and reactive (bottom) power delivered by the grid
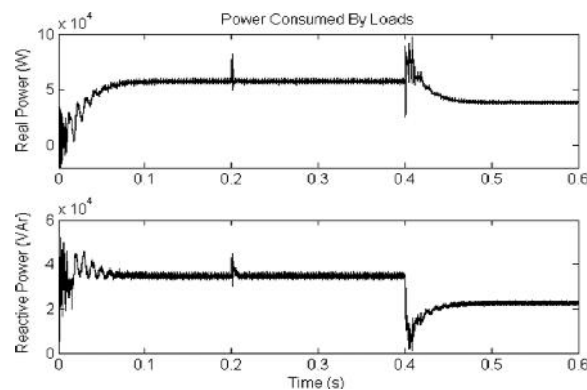

Figure 18. Real power delivered by SB

Figure 19. Real (top) and reactive (bottom) power consumed by loads

6. Conclusion

The role of Micro grid in penetration of DG's in the present utility network is discussed. Modelling of micro grid is a key aspect and the recent developments in the modelling of micro grid are presented in both grid-connected and autonomous mode. The proposed control techniques for the DG inverters based on a new MPC algorithm in order to reduce the overall computational time. DG inverters can compensate for load harmonic currents, hence power quality can be improved. Micro grid perform different operating conditions effectively thus increasing the overall reliability and stability of the micro grid.

References
[1]   IEEE Standards Coordinating Committee 21. IEEE Std.1547.4-2011:IEEE. *Guide for Design, Operation, and Integration of Distributed Resource Island Systems with Electric Power Systems.* 2011*.*
[2]   S Braithwait. Behaviour management. *IEEE Power and Energy Mag.* 2010; 8(3): 36-45.
[3]   N Jenkins, J Ekanayake, G Strbac. Distributed Generation. *IET*. London, U.K. 2009.

[4]   MY Zhai. Transmission characteristics of low-voltage distribution networks in China under the smart grids environment. *IEEE Trans. Power Del.* 2011; 26(1): 173-180.

[5]   Sun Hongbin, Tian Chunguang. Optimizing Multi-agent MicroGrid Resource Scheduling by Co-Evolutionary with Preference. *TELKOMNIKA Indonesian Journal of Electrical Engineering.* 2013; 11(12): 7222-7229.

[6]   GC Heffner, CA Goldman, MM Moezzi. Innovative approaches to verifying demand response of water heater load control. *IEEE Trans. Power Del.* 2006; 21(1): 1538-1551.

[7]   R Lasseter, J Eto, B Schenkman, J Stevens, H Vollkommer, D Klapp, E Linton, H Hurtado, J Roy. Certs micro grid laboratory test bed, and smart loads. *IEEE Trans. Power Del.* 2011; 26(1): 325-332.

[8]   A Molderink, V Bakker, MGC Bosman, JL Hurink, GJM Smit. Management and control of domestic smart grid technology. *IEEE Trans. Smart Grid.* 2010; 1(2): 109-119.

[9]   M Charkhgard, M Farrokhi. State-of-charge estimation for lithium-ion batteries using neural networks and EKF. *IEEE Trans. Ind. Electron.* 2010; 57(12): 4178-4187.

[10]   JA Macias, A Gomez. Self-tuning of Kalman filters for harmonic computation. *IEEE Trans. Power Del.* 2006; 21(1): 501–503.

[11]   Mian Xing, Ling Ji, Baiting Xu. Multiple Objective Optimizations for Energy Management System under Uncertainties. *TELKOMNIKA Indonesian Journal of Electrical Engineering.* 2013; 11(12): 7044-7051.

[12]   PK Ray, B Subudhi. Ensemble Kalman filter based power system harmonic estimation. *IEEE Transactions on Instrumentation and Measurement.* 2012; 61(12): 3216-3224.

[13]   P Mahat, Z Chen, B BakJensen. *Review of islanding detection methods for distributed generation.* In Proceedings of the 3rd International Conference on Deregulation and Restructuring and Power Technologies (DRPT '08). 2008: 2743-2748.

[14]   Kodanda Ram RBPUSB, M Venu Gopala Rao. Operation and Control of Grid Connected Hybrid AC/DC Microgrid using Various RES. *International Journal of Power Electronics and Drive System (IJPEDS).* 2014; 5(2): 195-202.